EPR Spectroscopy

International Edition: DOI: 10.1002/anie.201703154
German Edition: DOI: 10.1002/ange.201703154

Studying the Conformation of a Receptor Tyrosine Kinase in Solution by Inhibitor-Based Spin Labeling

Dongsheng M. Yin, Jeffrey S. Hannam, Anton Schmitz, Olav Schiemann, Gregor Hagelueken, and Michael Famulok**

Abstract: *The synthesis of a spin label based on PD168393, a covalent inhibitor of a major anticancer drug target, the epidermal growth factor receptor (EGFR), is reported. The label facilitates the analysis of the EGFR structure in solution by pulsed electron paramagnetic resonance (EPR) spectroscopy. For various EGFR constructs, including near-full-length EGFR, we determined defined distance distributions between the two spin labels bound to the ATP binding sites of the EGFR dimer. The distances are in excellent agreement with an asymmetric dimer of the EGFR. Based on crystal structures, this dimer had previously been proposed to reflect the active conformation of the receptor but structural data demonstrating its existence in solution have been lacking. More generally, our study provides proof-of-concept that inhibitor-based spin labeling enables the convenient introduction of site-specific spin labels into kinases for which covalent or tight-binding small-molecule modulators are available.*

Obtaining structural information on proteins in solution remains challenging, particularly when information on dynamic processes is desired. Although impressive progress is currently being made using single-particle cryo-electron microscopy, this technique is still limited to a few highly specialized laboratories and to proteins larger than about 100 kDa. While NMR-based methods are limited to proteins of small to medium size, pulsed electron paramagnetic resonance (EPR) spectroscopy is not restricted by these limitations. However, it requires the site-directed introduction of paramagnetic spin labels into the protein of interest, a process that is known as site-directed spin labeling (SDSL).[1] In the vast majority of SDSL approaches, the spin label is attached by modification of the thiol moiety of defined cysteine residues, producing nitroxide side chains coupled to the protein either through a disulfide or a thioether linkage. Thus, SDSL commonly requires the introduction of non-native cysteine residues at the desired sites while removing endogenous cysteines by serine or alanine substitutions. These requirements can be a drawback in cases where the mutations alter the structure or activity of the target protein. Therefore, spin-labeling strategies that are not based on cysteine mutation are of high interest. The use of non-natural amino acids as sites for labeling is such an approach. However, currently this method is restricted to proteins that can be expressed in *E. coli* or in an *E. coli*-derived cell-free expression system.[2] An attractive strategy not requiring amino acid substitutions is the use of spin label-bearing natural ligands, such as lipids or cofactors that target a distinct site in the protein of interest.[3] An analogous approach would be particularly promising for protein kinases, because a large variety of synthetic inhibitors targeting their ATP binding site with high specificity and affinity are available and can thus in principle be applied to label the protein. Moreover, more than 200 kinases, about 40 percent of the kinome, contain a cysteine residue in the ATP binding site, which can be used to covalently attach the inhibitor and thus the spin label, while avoiding the labeling of any other cysteine residues in the same protein.[4] Especially for receptor tyrosine kinases (RTKs) such as the epidermal growth factor receptor (EGFR), this approach appears a promising way to answer long standing questions about the conformational states of these important molecules in solution.[5] Therefore, we chose the EGFR to demonstrate the principal applicability of mutagenesis-independent SDSL for RTKs. In earlier efforts we had observed that replacing the cysteine residues in the EGFR kinase domain resulted in almost complete loss of activity (for an example, see the Supporting Information, Figure S1), indicative of structural changes resulting from the mutations, precluding traditional, mutagenesis-based SDSL for the EGFR. However, a large number of ATP-competitive small molecule inhibitors have been developed for the EGFR, some of which covalently target a cysteine residue in the ATP-binding site.[6]

Herein we report the development and application of an EPR spin label derived from the covalent type I EGFR inhibitor PD168393[7] (Supporting Information, Figure S2). We developed a variant of the synthesis described previously for the fluorophore-labeled version of PD168393[8] (Support-

[*] D. M. Yin, Dr. A. Schmitz, Prof. Dr. M. Famulok
Max Planck Fellow Chemical Biology
Center of Advanced European Studies and Research (caesar)
Ludwig-Erhard-Allee 2, 53175 Bonn (Germany)
E-mail: m.famulok@uni-bonn.de
D. M. Yin, Dr. J. S. Hannam, Dr. A. Schmitz, Prof. Dr. M. Famulok
LIMES Chemical Biology Unit
Rheinische Friedrich-Wilhelms-Universität Bonn
Gerhard-Domagk-Strasse 1, 53121 Bonn (Germany)
Prof. Dr. O. Schiemann, Dr. G. Hagelueken
Institute of Physical and Theoretical Chemistry
Rheinische Friedrich-Wilhelms-Universität Bonn
Wegelerstrasse 12, 53115 Bonn (Germany)
E-mail: hagelueken@pc.uni-bonn.de
Supporting information and the ORCID identification number(s) for the author(s) of this article can be found under: https://doi.org/10.1002/anie.201703154.

ing Information, Scheme S1). The synthesis follows standard procedures to 7-fluoroquinazoline **4** (Supporting Information, Scheme S1). Subsequently, Boc-ethanolamine was installed with a crown ether catalyzed *ipso*-substitution to give **5**. The acrylamide **7** was elaborated in a two-step procedure, firstly reacting aniline **6** with 3-chloropropionic acid chloride, followed by β-elimination with triethylamine. Finally, **1** (Figure 1 A) was obtained after Boc deprotection of **7** and

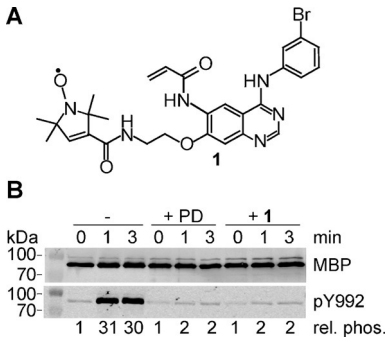

Figure 1. An inhibitor-derived EGFR EPR probe. A) To generate a covalently attached EPR probe, the irreversible EGFR inhibitor PD168393 was modified with the spin label 1-oxyl-2,2,5,5-tetramethylpyrroline-3-carboxylic acid via an ethanolamine spacer to yield **1**. B) The inhibitory activity of **1** was verified in an EGFR autophosphorylation assay in direct comparison with PD168393. Phosphorylated MBP-EGFR-ICD998 (pY992) was visualized by anti-EGFR(pY992) antibody and total amount of MBP-EGFR-ICD998 (MBP) by anti-MBP antibody. PD: PD168393. rel. phos.: phosphorylation levels at 1 and 3 min relative to the value at 0 min (set as 1 for each sample).

reaction with commercially available spin label **8**. The short ethanolamine linker was chosen to reduce the steric flexibility of the spin label relative to the inhibitor moiety, which should result in sharper distance distributions.

To verify that **1** retained the inhibitory function of PD168393, the ability of **1** to inhibit the EGFR kinase activity was determined. For this purpose, a truncated version of the intracellular domain (ICD) of the EGFR (EGFR-ICD998) was purified as a fusion protein with maltose-binding protein (MBP) as carrier (for details on the constructs see the Supporting Information, Figure S3). Owing to the presence of the juxtamembrane segment of the EGFR, which is required for efficient receptor dimerization and activation,[9] the fusion protein is active in a cell-free autophosphorylation assay. Both, PD168393 and **1** reduced the autophosphorylation of the construct to the same extent (Figure 1 B).

MBP-EGFR-ICD998 labeled with **1** was then used for pulsed electron–electron double resonance (PELDOR) measurements. Crystal structures for the full-length ICD are currently not available. Instead, an EGFR construct comprising amino acids 645–998 was the first to be crystallized[10] and extensively characterized by crystallography, including a structure covalently linked to PD168393 (PDB: 2J5F).[8] In this structure, the EGFR was observed in an asymmetric dimer, also known as the active conformation.[11] The EGFR kinase domain also crystallizes in a symmetric dimer that has been proposed to reflect the inactive conformation.[11] In the inactive and active EGFR dimer structures, the binding sites of **1** are about 30 Å or about 65 Å apart, respectively (Figure 2 A). Such a large difference in distances is well-suited to distinguish the active and inactive conformation of the EGFR by PELDOR spectroscopy. To verify that the protein was efficiently labeled with **1**, we conducted cw-X-band EPR measurements (Figure 2 C) and determined an average spin-labeling degree of at least 80 %, in accordance with the inhibition of autophosphorylation (Figure 1 B).

The Q-band PELDOR time trace for **1**-labeled MBP-EGFR-ICD998 revealed a slow initial decay and a pronounced modulation of the echo intensity with an average ($n = 3$) modulation depth of 26 % (green in Figures 2 B,C; see

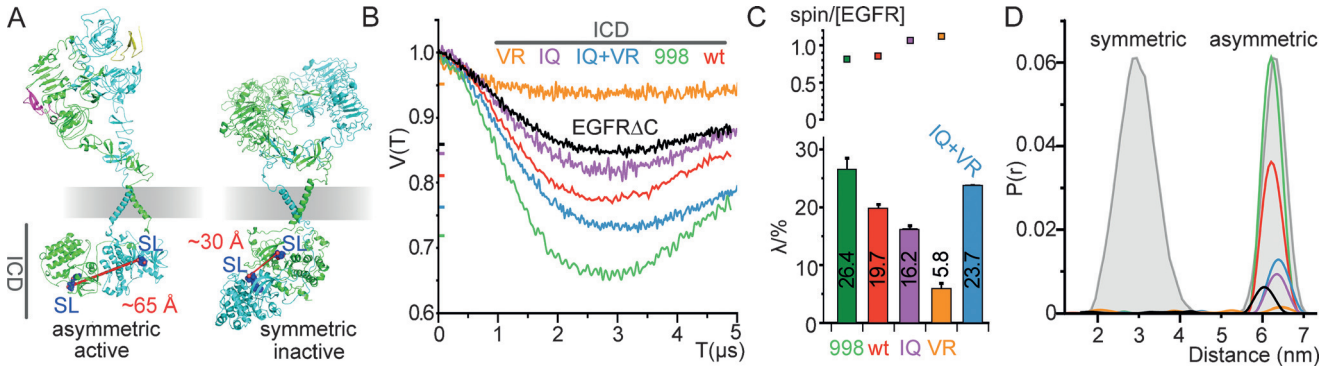

Figure 2. PELDOR on **1**-labeled EGFR constructs. A) The previously proposed[15] asymmetric (active) and symmetric (inactive) EGFR dimers are shown as cartoon models. The two individual monomers of each dimer are colored blue and green and the position of the membrane is indicated as gray shading. The two EGF ligands on the extracellular domain of the asymmetric dimer are shown as magenta and yellow cartoons. Models of two **1** spin labels (SL) in each dimer are shown as blue spheres and the distance vectors between them as red lines. B) Background-corrected PELDOR time traces of the EGFR constructs indicated on the top (see the Supporting Information, Figure S4 for raw data). The gray line marks constructs that only contain the ICD. The modulation depth of each time trace is marked on the *y* axis (as $V_\lambda = 1-\lambda$). C) Modulation depth λ in percent (lower *y*-axis) and spin labeling efficiency (upper *y*-axis) for EGFR-ICD constructs. Note that IQ + VR is a mixture of the two individual constructs and thus no labeling efficiency is given. The coloring is the same as in (B). D) Distance distributions calculated from (B) using DeerAnalysis2016. The samples are colored according to (B) and the mtsslWizard predictions for the symmetric and asymmetric states are represented by gray shading. VR: MBP-EGFR-ICD998(V924R), IQ: MBP-EGFR-ICD998(I682Q), 998: MBP-EGFR-ICD998, wt: MBP-EGFR-ICD.

the Supporting Information, Figure S4 for the uncorrected PELDOR time traces). Analysis of the time trace with DeerAnalysis2016[12] resulted in a distance distribution with a well-defined peak at 6.3 nm (Figure 2D). To accurately compare this distance to the available structures of EGFR, while accounting for the flexibility of the attached nitroxide group (Figure 1A), **1** was implemented into the in silico spin labeling software mtsslWizard.[13] Using this program, the spin–spin distance was predicted for both the active- and inactive conformations of the EGFR. Figure 2D shows that the experimental distance distribution fits almost perfectly to the distance that was predicted for the asymmetric active dimer (Figure 2D, green). Interestingly, no significant amount of **1**-labeled MBP-EGFR-ICD998 in the symmetric inactive conformation was detectable (Figure 2D). The cw-X-band spectra of **1**-labeled EGFR indicated a rather rigid spin label. For this reason, we investigated, whether the PELDOR signal was orientation selective. Time traces with different frequency offsets between pump and probe pulses were recorded and the Pake patterns calculated. This analysis did not reveal evidence for orientation selectivity (Supporting Information, Figure S5). A possible reason for this combination of broad cw-X-band spectra and absence of orientation selectivity would be multiple distinct orientations of the spin label, where each orientation is individually stabilized by interactions with the protein surface.

The region distal to the kinase domain, the so-called C-terminal tail, has been described as an autoinhibitory region in the EGFR.[14] The lack of most of this region in our construct might shift the equilibrium of inactive and active states to the latter. Therefore, we repeated the measurement with MBP-EGFR-ICD, that is, the full-length ICD containing the complete autoinhibitory region (Figure 2B, red). Also for this construct, we found exclusively the asymmetric, active-like dimer (Figure 2D). Interestingly, this construct reproducibly led to PELDOR time traces with a lower modulation depth compared to the C-terminally truncated EGFR-ICD998 construct (Figures 2B,C). Since the labeling efficiencies (Figure 2C, upper *y*-axis), as well as the inhibition of the autophosphorylation (Supporting Information, Figure S6) were comparable between the two samples, this result may be explained by an increased amount of monomeric EGFR-ICD compared to EGFR-ICD998. Further experiments will be needed to clarify whether this observation is of any functional relevance.

The spin–spin distance of 6.3 nm for the **1**-labeled EGFR-ICD dimer fits perfectly the distance deduced from models of the asymmetric dimer. Nevertheless, it could result from a dimer in another conformation having accidentally the same interspin distance. Therefore, we analyzed MBP-EGFR-ICD998(I682Q) and MBP-EGFR-ICD998(V924R), two EGFR mutants having a reduced ability to form the asymmetric dimer, due to point mutations in the interface area.[11] The PELDOR time traces of both mutants showed reduced modulation depths of only 6% for V924R and 16% for I682Q (Figures 2B,C, orange and purple, respectively). The reduced modulation depths are not due to inefficient labeling as shown by cw-X-band EPR measurements (Figure 2C) and inhibition studies (Supporting Information, Figure S6). Analyzing the remaining dipolar signal with DeerAnalysis2016 revealed the same distance as found for the "wild-type" constructs (Figure 2D). Correspondingly, some residual activity of the mutants was found in the autophosphorylation assay (Supporting Information, Figure S6). Mixing MBP-EGFR-ICD998(I682Q) and MBP-EGFR-ICD998(V924R) at equimolar concentrations should regain the ability to form an asymmetric dimer.[11] Indeed, we observed a significantly increased average modulation depth of 24% (vs. 26% for MBP-EGFR-ICD998) and the same active dimer distance as for the wild-type sample. These findings support the view that the measured 6.3 nm interspin distance indeed derives from the asymmetric dimer as found in crystal structures. Our results confirm that the interface mutations severely limit the ability of EGFR to form the active dimer. However, they do not shift the equilibrium to the symmetric dimer but rather to a monomeric form of EGFR. These findings are in accordance with cellular studies showing that full-length EGFR containing either the I682Q or V924R mutation had a drastically reduced ability to form dimers even when dimerization was stimulated by treatment of the cells with EGF.[14] In contrast however, the isolated EGFR(V924R) kinase domain crystallizes in the form of the symmetric dimer.[9a]

Therefore, to investigate the effect of the mutants on dimerization by an EPR-independent method, we analyzed the PELDOR samples by analytical gel filtration. MBP-

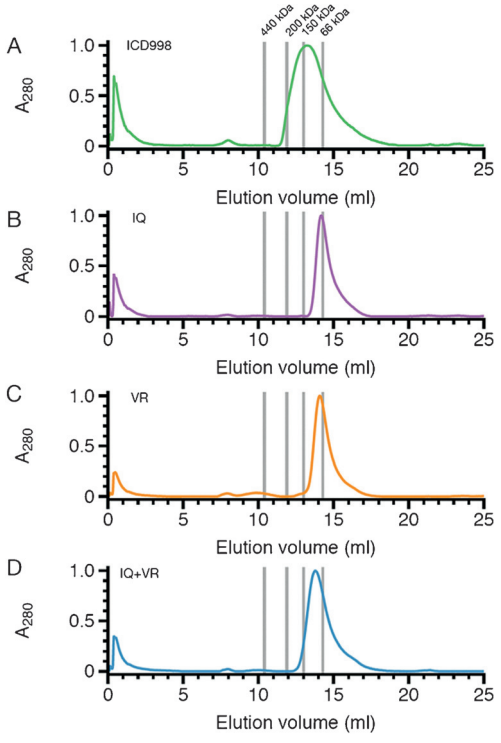

Figure 3. Analytical gel filtration of the PELDOR samples shown in Figure 2. A) MBP-EGFR-ICD998. B) MBP-EGFR-ICD998(I682Q). C) MBP-EGFR-ICD998(V924R). D) 1:1 mixture of I682Q and V924R mutants. For each panel, the absorption at 280 nm was normalized to values between 0 and 1 to allow easier comparison of the traces. Vertical lines indicate the peak elution volumes of the calibration standards.

EGFR-ICD998 produced a relatively broad peak (Figure 3A). The maximum of the peak eluted at the position of the 150 kDa calibration standard fitting the theoretical mass of the dimer of 160 kDa. In contrast, the two mutants I682Q and V924R produced sharper peaks at higher elution volumes (14.1 mL for both mutants), fitting the elution volume of the EGFR kinase monomer (Figure 3B,C). The I682Q + V924R mixture showed a slightly broadened peak (compared to I682Q or V924R alone) at an elution volume of 13.8 mL (Figure 3D). The broadening can be explained by a weak interaction between the monomers, leading to an overall slightly faster passage through the column.[16] This explanation is supported by the PELDOR result of the I682Q + V924R mixture, where an increased modulation depth, as compared to the individual proteins, but a slightly reduced modulation depth, as compared to wild-type EGFR, was observed (Figure 2C). Thus, the PELDOR as well as the gel filtration measurements show that **1**-labeled MBP-EGFR-ICD998(V924R) exists mainly as monomer in solution.

Next, we measured the interspin distance distribution of EGFRΔC, a construct containing the complete extracellular and transmembrane domains (Supporting Information, Figure S3). Using negative staining electron microscopy, stabilization of the asymmetric dimer by PD168393 has been reported for a very similar construct.[17] EGFRΔC, purified in Triton-X 100 micelles, showed EGF-dependent autophosphorylation, which was inhibited by **1** (Supporting Information, Figure S7). The PELDOR time trace of **1**-labeled EGFRΔC is shown in Figure 2B (black) and indeed looks very similar to the time traces of the ICD constructs. Note that the modulation depth of this construct cannot be compared to those of the other constructs because for technical reasons the labeling was done differently (see the Supporting Information, Methods). This does, however, not affect the determination of the interspin distances. Using DeerAnalysis2016 an interspin distance fitting the asymmetric dimer was calculated (Figure 2D).

In summary, our data provide strong structural evidence that in solution, the **1**-labeled EGFR kinase domain adopts the conformation of the asymmetric dimer found in crystals. Interestingly, our results suggest that the **1**-bound EGFR either forms an asymmetric, active-like dimer or no dimer at all. In none of our measurements, any significant signals fitting the symmetric, inactive dimer were found. There are at least two possible explanations for its apparent absence: 1) Compound **1** might simply not fit into the active site of the symmetric EGFR kinase dimer. To check this, we modeled **1** into the active sites of both dimers with mtsslWizard and found that it fits similarly well in both cases (Supporting Information, Figure S8); 2) binding of **1** may alter the symmetric/asymmetric equilibrium by stabilization of the asymmetric dimer. This might correspond to the finding that helix αC adopts the active, inward-rotated conformation in the co-crystal of the EGFR kinase domain with PD168393.[8] This conformation of helix αC is known to be stabilized by the asymmetric dimer.[18]

In conclusion, we have developed a kinase inhibitor-derived EPR spin label for the EGFR. More generally, by employing a spin-labeled, covalent RTK inhibitor we have established a versatile method to analyze the conformation of RTKs by EPR spectroscopy in solution. Note that there are many small molecule modulators available that have different binding modes as compared to PD168393 and thus could serve as spin-label vehicles to study different states of these important receptors. We envision that in the future, a combination of SDSL and spin-label bearing small molecules will greatly facilitate studies on protein dynamics in solution and in cells by EPR methods.

Acknowledgements

The Max-Planck-Society and Bonn University supported this work through a Max-Planck-Fellowship to M.F. We thank Y. Aschenbach-Paul, V. Fieberg, and F. Duthie for technical assistance. We thank E. Schubert for collecting some of the cw-X-band spectra.

Conflict of interest

The authors declare no conflict of interest.

Keywords: covalent inhibitor spin probe · epidermal growth factor receptor · EPR spectroscopy · PELDOR · spin labels

How to cite: *Angew. Chem. Int. Ed.* **2017**, *56*, 8417–8421
Angew. Chem. **2017**, *129*, 8537–8541

[1] a) J. P. Klare, H.-J. Steinhoff, *Photosynth. Res.* **2009**, *102*, 377–390; b) W. L. Hubbell, D. S. Cafiso, C. Altenbach, *Nat. Struct. Mol. Biol.* **2000**, *7*, 735–739.
[2] a) M. R. Fleissner, E. M. Brustad, T. Kalai, C. Altenbach, D. Cascio, F. B. Peters, K. Hideg, S. Peuker, P. G. Schultz, W. L. Hubbell, *Proc. Natl. Acad. Sci. USA* **2009**, *106*, 21637–21642; b) E. H. Abdelkader, A. Feintuch, X. Yao, L. A. Adams, L. Aurelio, B. Graham, D. Goldfarb, G. Otting, *Chem. Commun.* **2015**, *51*, 15898–15901.
[3] a) B. J. Gaffney, M. D. Bradshaw, S. D. Frausto, F. Wu, J. H. Freed, P. Borbat, *Biophys. J.* **2012**, *103*, 2134–2144; b) B. Joseph, A. Sikora, E. Bordignon, G. Jeschke, D. S. Cafiso, T. F. Prisner, *Angew. Chem. Int. Ed.* **2015**, *54*, 6196–6199; *Angew. Chem.* **2015**, *127*, 6294–6297.
[4] J. Zhang, P. L. Yang, N. S. Gray, *Nat. Rev. Cancer* **2009**, *9*, 28–39.
[5] I. N. Maruyama, *Cells* **2014**, *3*, 304–330.
[6] Q. Liu, Y. Sabnis, Z. Zhao, T. Zhang, S. J. Buhrlage, L. H. Jones, N. S. Gray, *Chem. Biol.* **2013**, *20*, 146–159.
[7] D. W. Fry, A. J. Bridges, W. A. Denny, A. Doherty, K. D. Greis, J. L. Hicks, K. E. Hook, P. R. Keller, W. R. Leopold, J. A. Loo, D. J. McNamara, J. M. Nelson, V. Sherwood, J. B. Smaill, S. Trumpp-Kallmeyer, E. M. Dobrusin, *Proc. Natl. Acad. Sci. USA* **1998**, *95*, 12022–12027.
[8] J. A. Blair, D. Rauh, C. Kung, C.-H. Yun, Q.-W. Fan, H. Rode, C. Zhang, M. J. Eck, W. A. Weiss, K. M. Shokat, *Nat. Chem. Biol.* **2007**, *3*, 229–238.
[9] a) N. Jura, N. F. Endres, K. Engel, S. Deindl, R. Das, M. H. Lamers, D. E. Wemmer, X. Zhang, J. Kuriyan, *Cell* **2009**, *137*, 1293–1307; b) M. Red Brewer, S. H. Choi, D. Alvarado, K. Moravcevic, A. Pozzi, M. A. Lemmon, G. Carpenter, *Mol. Cell* **2009**, *34*, 641–651.

[10] J. Stamos, M. X. Sliwkowski, C. Eigenbrot, *J. Biol. Chem.* **2002**, *277*, 46265 – 46272.
[11] X. Zhang, J. Gureasko, K. Shen, P. A. Cole, J. Kuriyan, *Cell* **2006**, *125*, 1137 – 1149.
[12] G. Jeschke, V. Chechik, P. Ionita, A. Godt, H. Zimmermann, J. Banham, C. R. Timmel, D. Hilger, H. Jung, *Appl. Magn. Reson.* **2006**, *30*, 473 – 498.
[13] G. Hagelueken, R. Ward, J. H. Naismith, O. Schiemann, *Appl. Magn. Reson.* **2012**, *42*, 377 – 391.
[14] E. M. Bublil, G. Pines, G. Patel, G. Fruhwirth, T. Ng, Y. Yarden, *FASEB J.* **2010**, *24*, 4744 – 4755.
[15] A. Arkhipov, Y. Shan, R. Das, N. F. Endres, M. P. Eastwood, D. E. Wemmer, J. Kuriyan, D. E. Shaw, *Cell* **2013**, *152*, 557 – 569.
[16] F. J. Stevens, M. Schiffer, *Biochem. J.* **1981**, *195*, 213 – 219.
[17] L.-Z. Mi, C. Lu, Z. Li, N. Nishida, T. Walz, T. A. Springer, *Nat. Struct. Mol. Biol.* **2011**, *18*, 984 – 989.
[18] R. Bose, X. Zhang, *Exp. Cell Res.* **2009**, *315*, 649 – 658.

Manuscript received: March 27, 2017
Version of record online: June 19, 2017

